JOURNAL OF MAGNETIC RESONANCE IMAGING 35:1462–1471 (2012)

Original Research

Four-Dimensional Phase Contrast MRI With Accelerated Dual Velocity Encoding

Elizabeth J. Nett, MS,[1]* Kevin M. Johnson, PhD,[1] Alex Frydrychowicz, MD,[2] Alejandro Munoz Del Rio, PhD,[2] Eric Schrauben, BS,[1] Christopher J. Francois, MD,[2] and Oliver Wieben, PhD[1,2]

Purpose: To validate a novel approach for accelerated four-dimensional phase contrast MR imaging (4D PC-MRI) with an extended range of velocity sensitivity.

Materials and Methods: 4D PC-MRI data were acquired with a radially undersampled trajectory (PC-VIPR). A dual V_{enc} (dV_{enc}) processing algorithm was implemented to investigate the potential for scan time savings while providing an improved velocity-to-noise ratio. Flow and velocity measurements were compared with a flow pump, conventional 2D PC MR, and single V_{enc} 4D PC-MRI in the chest of 10 volunteers.

Results: Phantom measurements showed excellent agreement between accelerated dV_{enc} 4D PC-MRI and the pump flow rate ($R^2 \geq 0.97$) with a three-fold increase in measured velocity-to-noise ratio (VNR) and a 5% increase in scan time. In volunteers, reasonable agreement was found when combining 100% of data acquired with V_{enc} = 80 cm/s and 25% of the high V_{enc} data, providing the VNR of a 80 cm/s acquisition with a wider velocity range of 160 cm/s at the expense of a 25% longer scan.

Conclusion: Accelerated dual V_{enc} 4D PC-MRI was demonstrated in vitro and in vivo. This acquisition scheme is well suited for vascular territories with wide ranges of flow velocities such as congenital heart disease, the hepatic vasculature, and others.

Key Words: phase contrast; flow quantification; vascular hemodynamics; velocity mapping; rapid imaging
J. Magn. Reson. Imaging 2012;35:1462–1471.

PHASE CONTRAST MRI (PC MRI) can obtain quantitative blood flow, peak velocity and other hemodynamic indicators of cardiovascular dysfunction. These measurements can be used to grade the severity of stenoses, quantify valvular regurgitation, or calculate shunt fractions (1,2). Traditionally, clinical use of PC MR has been limited to 2D cine imaging with one-directional (through-plane) velocity encoding due to long imaging times for cardiac gated, volumetric (three-dimensional [3D]) PC acquisitions with three-directional velocity encoding. However, recent advances in hardware and imaging techniques have made such acquisitions, sometimes referred to as "4D MR Flow" or "4D PC-MRI" feasible in clinically relevant scan times of approximately 12–20 minutes for cardiac scans (3–6). 4D PC-MRI allows for comprehensive assessment of cardiovascular function, providing volumetric anatomical and quantitative hemodynamic information throughout the cardiac cycle (3,4,6–11).

One challenge of phase contrast MR and 4D PC-MRI in particular is the choice of the optimal velocity encoding setting (V_{enc}). The V_{enc} determines the dynamic range of the velocity map obtained from the acquisition. If the V_{enc} is set too low, phase aliasing, also known as phase wrapping, occurs in regions of velocities exceeding the V_{enc}, thereby rendering quantitative measurements difficult or impossible. If the V_{enc} is set too high, the velocity-to-noise ratio (VNR), itself inversely proportional to the V_{enc} setting, suffers. The increased noise will lead to erroneous velocity readings, particularly in regions of slow flow. Therefore, the V_{enc} must be chosen close to but higher than the highest expected velocity of interest in the chosen imaging plane or volume. Optimal V_{enc} settings are not predictable and particularly difficult to determine for acquisitions with volumetric coverage where a large range of velocities is expected. A single optimal V_{enc} setting might not exist, especially in difficult situations imaging complex flow patterns or vascular territories, such as in arteriovenous malformations, surgical alteration after congenital heart disease, or the hepatic vasculature with its dual arterial and portal venous blood supply.

[1]Department of Medical Physics, University of Wisconsin, Madison, Wisconsin, USA.
[2]Department of Radiology, University of Wisconsin, Madison, Wisconsin, USA.
Contract grant sponsor: NIH; Contract grant number: R01HL072260.
*Address reprint requests to: E.J.N., University of Wisconsin – Madison, Department of MR/CT Research, Wisconsin Institutes for Medical Research (WIMR), 1111 Highland Avenue, Madison, WI 53705-2275. E-mail: janus@wisc.edu
Received April 20, 2011; Accepted December 15, 2011.
DOI 10.1002/jmri.23588
View this article online at wileyonlinelibrary.com.

Dynamic range issues could be addressed with the acquisition of two or more separate scans with different V_{enc} settings. Multiple V_{enc} encoding schemes extend the velocity encoding range of the scan but also increase the scan time. For one-directional flow encoding, two different V_{enc}s can be acquired using 3 flow encodings (reference and two velocity encoded), which requires a 50% increase in scan time. For three-directional flow encoding, a single V_{enc} acquisition requires at least four acquisitions (a reference and three velocity encoded acquisitions) and each additional V_{enc} requires three to four additional flow encodings. Further prolonging the scan time, the bipolar gradients of the velocity encoded scans extend the echo time (TE) and repetition time (TR) especially in cases of low velocity encoding setting, in which the TR can almost double. The additional time required for multiple scans with different V_{enc}s would often lead to prohibitively long imaging times for 4D PC-MRI.

Rather than acquiring multiple V_{enc}s, phase errors in a scan with a too low V_{enc} setting could be corrected with automatic phase unwrapping (12,13) but these algorithms often fail in large aliased regions or areas of multiple wrapping. In addition, velocities measured with lower V_{enc}s are more susceptible to errors from intra-voxel dephasing (14) and longer echo times (TE). Due to scan time penalties and diminishing gains, alternative velocity encoding schemes have been investigated (15–19). One such encoding scheme, a 5-point balanced technique, was shown to improve VNR by 60% for a 25% increase in scan time. However, the ratio between the higher and lower velocity encoding are not flexible with this scheme.

In this study, a dual V_{enc} (dV_{enc}) reconstruction approach on the basis of phase contrast Vastly undersampled Projection Reconstruction (PC VIPR) data was explored. PC VIPR is a 3D radially undersampled phase contrast sequence with three-directional velocity encoding (7). Without modification, this dual V_{enc} acquisition would double the scan time due to additional high V_{enc} encoding steps. To minimize the scan time penalty from added encoding steps, the effect of additional radial undersampling applied to the high V_{enc} acquisition has been explored, possibly introducing undersampling artifacts yet maintaining the spatial resolution (20).

The aim of this study was two-fold: (i) to evaluate the accuracy of an accelerated dV_{enc} PC VIPR acquisition and reconstruction in phantom experiments and (ii) to study the in vivo utility of dV_{enc} PC VIPR in 10 healthy volunteers by evaluating the tradeoffs between savings in scan times, VNR, and velocity measurements. Specifically, we compared dV_{enc} PC VIPR data with various acceleration factors to a standard "single" V_{enc} PC VIPR acquisition and 2D phase contrast acquisitions as the intrinsic and clinical reference. The comparison included the VNR of the resulting image, the measured blood flow parameters peak velocity [cm/s] and flow volume [mL] in five locations of the thoracic vasculature, and the clinically relevant ratio of pulmonic (Qp) to systemic (Qs) blood flow.

MATERIALS AND METHODS

Dual V_{enc} Theory

The V_{enc} is defined as the velocity which corresponds to a phase shift of π and is inversely proportional to the first moment difference between two flow encodings (Δm_1):

$$V_{enc} = \frac{\pi}{|\gamma \Delta m_1|} \quad [1]$$

Subsequently, the velocity can be determined using the relationship:

$$v = \frac{\varphi}{\pi} V_{enc} \quad [2]$$

Where ϕ is the phase difference between two flow encodings. If the ϕ velocity is greater than the chosen V_{enc}, ϕ will be greater than π and velocity aliasing will occur. The VNR is a function of the V_{enc}:

$$VNR \propto \frac{SNR}{V_{enc}} \quad [3]$$

If the V_{enc} is too high, the VNR may not be sufficient to make accurate measurements in slow flow regions.

Dual V_{enc} reconstruction algorithms combine data from high and low V_{enc} acquisitions to reduce the tradeoffs between VNR and dynamic range. The high V_{enc} is chosen high enough to avoid phase wrapping errors. Estimated velocities, v_{est}, are obtained from the high V_{enc} data set and can be used to identify phase aliasing in the low V_{enc} image and calculate the number of phase wraps:

$$n = NI\left(\frac{Av_{est} - \varphi}{2\pi}\right) \quad [4]$$

where NI is the nearest integer function and A is the matrix containing the Δm_1 values for each encoding in rows. The unaliased phase in the low V_{enc} data is calculated using n:

$$\varphi_{unaliased} = \varphi + 2\pi n \quad [5]$$

This unaliased phase can then be used to calculate the velocity. The relationship between phase and velocity is:

$$v = A^{-1}\varphi \quad [6]$$

where v is the vector of velocities. Because the nearest integer function is insensitive to small deviations, the noise in the final image is dominated by the low V_{enc}, and without intra-voxel dephasing errors, the VNR improvement is proportional to the high-to-low V_{enc} ratio (21). In this study, to minimize the scan time penalty from added encoding steps, additional radial undersampling was applied to high V_{enc} data before the dual V_{enc} reconstruction. Although undersampling introduces errors in the high V_{enc} acquisition, these errors in the estimated velocities need to be greater than the low V_{enc} to cause errors in the final estimation.

Table 1
Protocol Parameters for Velocity Encoded MR Acquisitions in a Flow Phantom and Volunteer Study for a Volumetric, Radially Undersampled Acquisition (PC VIPR), and the Conventional 2D PC Acquisition

	In vitro PC VIPR	In vivo PC VIPR	In vivo 2D PC
Repetition time (ms)	6.6-7.0	6.2-6.6	5.4-5.5
Echo time (ms)	2.3-2.7	2-2.5	3.1-3.2
Flip angle (degrees)	10	10	30
Bandwidth (kHz)	125	125	62.5
Field of view (cm)	24x24	32x32	35x35
Slice thickness (mm)	0.94	1.25	6
Matrix size	256x256x256	256x256x256	256x160
No. of projections	10,000	15,000	NA
Acquisition length	5-6 min	12-13 min	22 heart beats
Velocity encodings (cm/s)	40,80,160	40,80,160	80-160
Undersampling Factor	10	7	NA

MR Imaging

Phantom and volunteer imaging was performed on a clinical 3T system (Discovery MR 750, GE Healthcare, Waukesha, WI) with a maximum gradient strength of 50 mT/m and a maximum slew rate of 200 mT/m/ms. Sequence details are summarized in Table 1. No contrast agent was administered for phantom or volunteer acquisitions. For each exam, three separate single V_{enc} PC VIPR scans were acquired for both phantom and volunteer experiments: a high V_{enc} and two low V_{enc}s all with four-point balanced (Hadamard) flow encoding and the same number of acquired projection angles. To simulate accelerated dual V_{enc}, high V_{enc} images were retrospectively reconstructed with varying degrees of additional radial undersampling. Dual V_{enc} images were generated by unwrapping each low V_{enc} image with the high V_{enc} images. A schematic diagram of the in vivo accelerated dual V_{enc} reconstruction is shown in Figure 1. Different high and low V_{enc}s settings were chosen for in vitro and in vivo scans to best match the velocities in those studies.

In Vitro Study

Study Design

Accelerated dual V_{enc} PC VIPR was validated using a MR compatible flow pump (CompuFlow 1000 MR, Shelley Medical Imaging Technologies, London, ON, CA) placed in the center of a quadrature head coil. The flow phantom consisted of one tube with an inner diameter of 7.9 mm and was looped in the bore such that two tube segments with opposing flows were within the coil. Each of these tube segments was permanently surrounded by a closed plastic pipe-like structure filled with doped water to minimize susceptibility artifacts and increase the coil loading. The tube was filled with blood-mimicking fluid (Shelley Medical Imaging Technologies, London, ON, CA) and connected to the flow pump. Flow was only measured in one of the tubes. Flow rates were chosen to match the observed in vivo range of venous and arterial blood flow velocities: flow rates of 8 mL/s, 12 mL/s, 18 mL/s, and 24 mL/s (mean velocities of ~16 cm/s, 24 cm/s, 36 cm/s, and 48 cm/s, maximum velocities of ~30, 60, 68, and 120 cm/s) in the tube. Three PC VIPR data sets were acquired with V_{enc}s of 30 cm/s, 60 cm/s, and 120 cm/s. At a pump flow rate of 12 mL/s, each acquisition was repeated for a subsequent velocity-to-noise (VNR) analysis. This analysis was performed at a single flow rate because the VNR ratios we compared can be expected to be on the same order at all the tested flow rates.

Reconstruction

Phantom data were acquired during constant flow and thus, three time-averaged, PC VIPR balanced-encoded data sets were reconstructed. Then, a dual V_{enc} reconstruction was accomplished by combing low V_{enc} (30 cm/s, 60 cm/s) and high V_{enc} (120 cm/s) acquisitions with the goal of generating aliasing free dual V_{enc} data. The phantom data were acquired with an undersampling factor of 10 with respect to radial Nyquist sampling and high V_{enc} data (120 cm/s) were reconstructed with 100%, 50%, 25%, 12%, 5%, and 2% of the acquired projections to mimic acquisitions of reduced scan times from a single data set. Each of

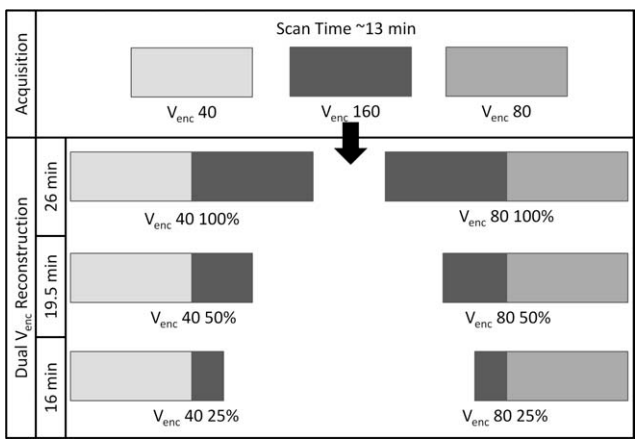

Figure 1. Schematic of acquisition and dual V_{enc} reconstruction. The parameters shown are those that were used in volunteers. Three, 12–13 min PC VIPR data sets are acquired with three V_{enc}s: one high V_{enc} (160 cm/s) and two low V_{enc}s (80, 40 cm/s). Dual V_{enc} images are reconstructed with a low V_{enc} data set and different percentages of the high V_{enc} data set. The undersampled high V_{enc} reconstruction mimics acquiring less high V_{enc} data.

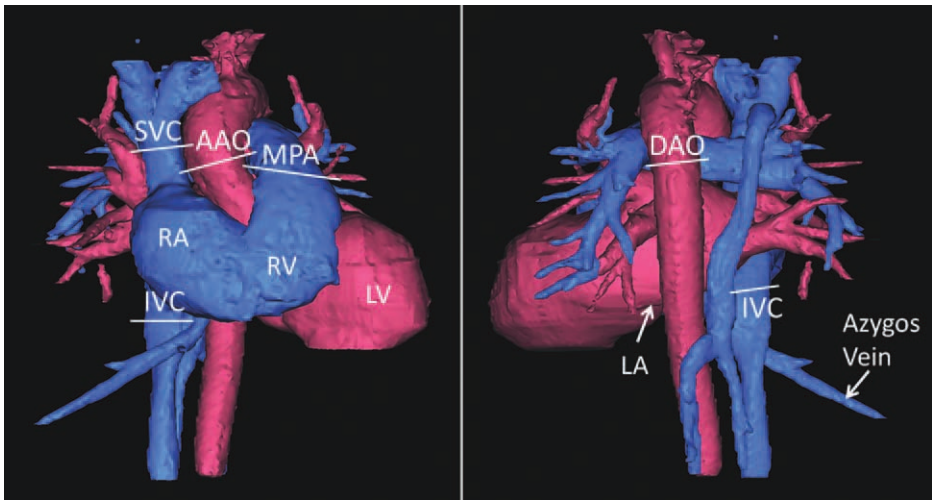

Figure 2. Slice locations analyzed in the comparison study. Volume rendering of the phase contrast angiogram derived from a PC VIPR exam was not part of the analysis. Arterial (red) and venous (blue) system have been segmented to facilitate orientation. Velocity and flow measurements were made in the ascending and descending aorta (AAO and DAO), main pulmonary artery (MPA), and superior and inferior vena cava (SVC and IVC). The left and right atrium (LA, RA) and ventricles (LV, RV) are labeled for reference.

the radially undersampled high V_{enc} data were used to correct each of the low V_{enc} (30 cm/s, 60 cm/s) images, hence, for each flow rate, there were a total of 12 dual V_{enc} PC VIPR images (six undersampling rates times two high and low V_{enc} combinations).

Flow and velocity measurements were made by placing identical regions of interest (ROIs) over all data using Matlab (Mathworks, Natick, MA) to guarantee comparable measurements. For the repeated experiments at 12 mL/s, VNR was calculated over an ROI as the ratio of the average velocity to the standard deviation in the subtracted image:

$$VNR = \frac{\sqrt{2}(\bar{v}_1 + \bar{v}_2)}{2std(v_1 - v_2)} \quad [7]$$

where v_1 and v_2 are the velocities in identical ROIs. VNR efficiency was calculated for each reconstructed dual V_{enc} image as the ratio of the VNR to the scan time relative to a standard four-point balanced-encoded PC VIPR image.

Statistical Analysis

The accuracy, VNR efficiency, and phase unwrapping of the dual V_{enc} PC reconstruction were tested. Linear regression analysis was used to assess the accuracy of dual V_{enc} PC VIPR by comparing measured and set pump flow rates. Marginal hypothesis tests of the null hypothesis that the intercept and slope equaled 0 and 1, respectively, were obtained. $P < 0.05$ (two-sided) was the criterion for statistical significance.

In Vivo Study

Study Design

Ten by case history healthy volunteers (27 ± 3 years old; range, 22–31 years; 75 ± 10 kg body weight; range, 54–82 kg; 8 men, 2 women) were scanned after approval of the local institutional review board (IRB) and obtaining written informed consent. Volunteer data were acquired with a 32-channel phased-array torso coil (NeoCoil, Pewaukee, WI). Bellow readings were performed for an acquisition gated to the breathing motion. The acceptance window was set to 50% (expiratory).

Three separate balanced, time-resolved velocity-encoded PC VIPR data sets were acquired with the V_{enc}s: 160 cm/s, 80 cm/s, and 40 cm/s. Each in vivo data set was acquired with an undersampling factor of approximately 7 with respect to radial Nyquist sampling. Each data set was reconstructed with approximately 20 time frames resulting in an undersampling factor of approximately 140 for each time frame with respect to Nyquist. Figure 2 shows the locations of prospectively gated, breath-hold, 2D PC acquisitions performed as intrinsic flow references: perpendicular to the ascending and descending aorta (AAO, DAO, respectively) at the level of the pulmonary artery (V_{enc} = 160 cm/s), main pulmonary artery (MPA) (V_{enc} = 120 cm/s), and superior and inferior vena cava (SVC, IVC) (V_{enc} = 80 cm/s). Following the recommendations of Chernobelsky et al., all 2D PC acquisitions were repeated in a static phantom to correct for residual phase errors (22).

Reconstruction

Retrospectively gated, time-resolved PC VIPR data were reconstructed using a temporal filter (23,24) as described for time-resolved contrast enhanced MRA with a 3D radial acquisition in (25). At the center of *k*-space, PC VIPR data were reconstructed with a time resolution similar to 2D PC (~40 ms). At the edge of *k*-space, the resolution was 20 TRs (~120 ms). In vivo high V_{enc} (160 cm/s) data were reconstructed with 100%, 50%, and 25% of the acquired projections resulting in undersampling factors for individual time frames of approximately 140, 280, and 560 with respect to Nyquist.

Velocity and Flow Measurements

PC VIPR images were reformatted into 2D slices in the exact locations of the 2D PC acquisitions with a home-built Matlab tool. Vessels boundaries were manually segmented on individual time frames using complex difference angiogram images to enable flow and velocity measurements.

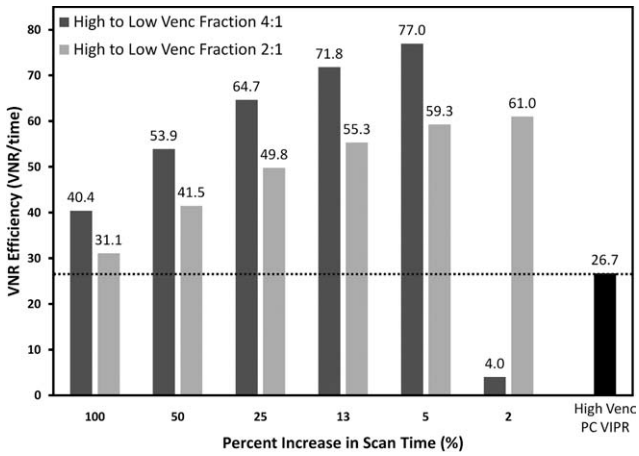

Figure 3. Relative gain in VNR efficiency of dual V_{enc} in comparison to a single/high V_{enc} PC VIPR scan. A marked increase in VNR efficiency can be achieved by decreasing undersampling expressed by relative scan times. With a 5% increase in scan time, the VNR efficiency can be increased from 26.7% to 77% (factor of 2.88) using a 4:1 ratio of high-to-low V_{enc} scan during the reconstruction. When only 2% of the high V_{enc} data is used to correct the low V_{enc} scan, the VNR plummets due to phase unwrapping errors.

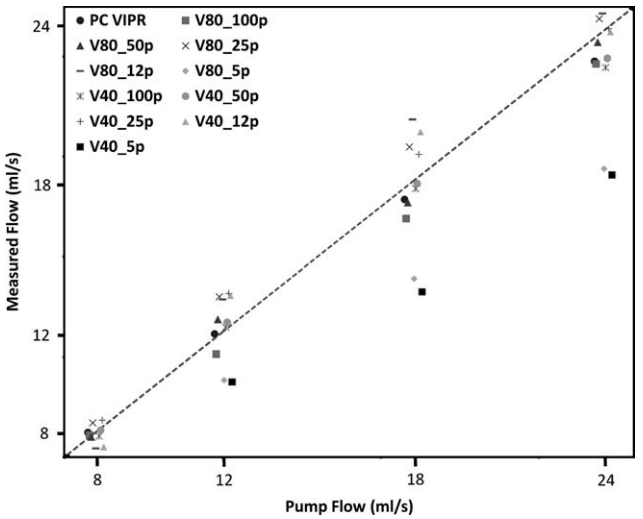

Figure 4. Flow rates measured with high V_{enc} PC VIPR and dual V_{enc} PC VIPR in a flow phantom programmed to deliver constant flow. Scatter was added around the set pump flow rates to allow for a better appreciation of the data. The dashed line marks the identity line. Overall, PC VIPR methods somewhat underestimated the flow rate but in most cases, flow rates measured agreed well with the programmed flow rates.

Statistical Analysis

The RR intervals were recorded as part of the retrospective gating scheme and subsequently analyzed for average and standard deviation for each V_{enc} acquisition (outliers from missed beats were excluded). Bland-Altman analysis was used to compare the flow volume, peak velocity, and the ratio of pulmonary to systemic blood flow (Q_p/Q_s) measured by all techniques. The Bland-Altman window was set to $\pm$ 2 SD of the observed differences of the compared values. The 2D PC was used as an internal reference and pair-wise comparisons were generated to compare individual PC VIPR data with 2D PC results. A single observer was used in this study.

RESULTS

In Vitro Study

Phantom experiments demonstrated the accuracy and VNR gains achievable with dual V_{enc} PC VIPR. Results from linear regression and VNR analysis are summarized in Figures 3 and 4 and Table 2. Phase wraps in low V_{enc} image are corrected with only 12% of the acquired high V_{enc} data. When only 5% and 2% of the high V_{enc} data are used in the reconstruction, more phase errors are introduced, particularly at the edge of the vessels.

Statistical Results

Linear regression analysis showed excellent accuracy for flow rates measured with dual V_{enc} PC VIPR. The flow rates measured with all PC VIPR techniques correlated extremely well with the programmed pump flow rate ($R^2 \geq 0.97$; $P \geq 0.06$ for both slope and intercept). Table 2 and Figure 4 summarize these results comparing flow rates measured with PC VIPR

Table 2
Results From Linear Regression Analysis Comparing Programmed Pump Flow With PC VIPR Measurements*

	Intercept	*P* value	Standard error	Slope	*P* value	Standard error	R^2
PCVIPR	−0.77	0.06	0.20	1.08	0.99	0.01	1.00
V80_100p	−0.17	0.81	0.59	1.07	0.99	0.04	1.00
V80_50p	−0.32	0.75	0.87	1.04	0.99	0.05	0.99
V80_25p	−0.80	0.50	0.98	0.99	0.99	0.06	0.99
V80_12p	0.68	0.73	1.72	0.90	0.65	0.10	0.98
V80_5p	0.73	0.64	1.36	1.23	1.43	0.10	0.98
V40_100p	−0.91	0.35	0.75	1.09	0.82	0.05	1.00
V40_50p	−1.05	0.24	0.64	1.08	0.80	0.04	1.00
V40_25p	−1.28	0.36	1.09	1.03	0.23	0.06	0.99
V40_12p	0.17	0.94	1.94	0.95	0.33	0.11	0.97
V40_5p	0.80	0.64	1.46	1.25	1.51	0.11	0.99

*The *P* values and standard errors associated with the intercept and slope are also reported, in all cases indicating that the null hypothesis (intercept = 0, slope = 1) cannot be disproven ($P > 0.05$). All flow measurements correlated extremely well with the pump flow rate.

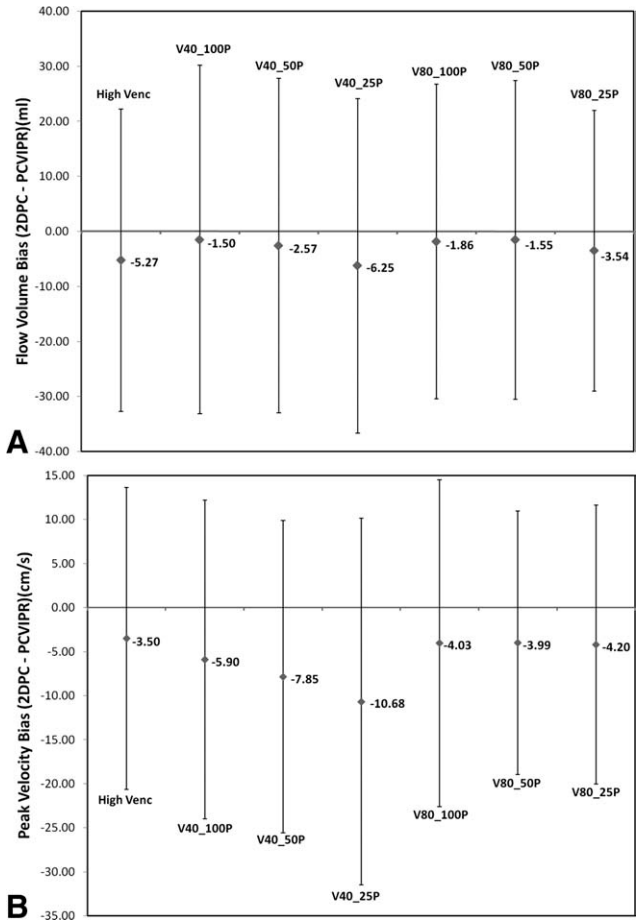

Figure 5. Summary of the results from Bland-Altman analysis comparing average (**A**) flow volume and (**B**) peak velocity measurements with 95% confidence intervals in high V_{enc} PC VIPR and dual V_{enc} PC VIPR with 2D PC. Flow volume [mL] was measured in the AAO, DAO, MPA, SVC, and IVC. Peak velocity was only measured in the arterial system (AAO, DAO, and MPA) because peak venous velocities are often difficult to define. The flow volumes and peak velocities measured with PC VIPR techniques are lower than those measured by 2D PC in most cases. This is most likely a result of the temporal filtering used in the PC VIPR reconstruction.

to the programmed pump flow rate. Overall, PC VIPR methods somewhat underestimated the flow rate but in most cases, flow rates measured agreed well with the programmed flow rates.

In Figure 5, the gains in VNR efficiency achieved with dual V_{enc} PC VIPR are displayed. With a dual V_{enc} reconstruction, it is possible to achieve a higher VNR efficiency than with single V_{enc} PC VIPR. VNR efficiency increases with higher undersampling until velocity errors from the high V_{enc} acquisition cause errors in the phase unwrapping. VNR efficiencies are lower for a high-to-low V_{enc} ratio of 2 to 1 than 4 to 1. With a high-to-low V_{enc} ratio of 4 to 1, it is possible to obtain a three-fold gain in VNR with a 5% increase in scan time. With a high-to-low V_{enc} ratio of 2 to 1, a two-fold increase in VNR can be obtained at the cost of only 2% increase in scan time.

In Vivo Study

Results of the volunteer study demonstrated the feasibility of dual V_{enc} PC VIPR reconstruction on in vivo acquired data. Results from statistical analysis comparing dual V_{enc} PC VIPR, balanced-encoded PC VIPR and 2D PC are summarized in Figures 5 and 6. Example single V_{enc} and dual V_{enc} PC VIPR images are shown in Figure 7. The dual V_{enc} images appear to have higher VNR compared with the high V_{enc} images and most of the velocity aliasing from the low V_{enc} acquisition is corrected with 100% and 50% of the acquired high V_{enc} projections. With a high-to-low V_{enc} ratio of 2:1, 25% of the high V_{enc} data is sufficient to remove aliasing. However, with a high-to-low V_{enc} ratio of 4:1, significant phase errors remain in the vessels when only 25% of the high V_{enc} data is used for unwrapping.

Statistical Results

Figure 5 summarizes the results of Bland-Altman analysis comparing average flow volume and peak velocity measurements with 95% confidence intervals measured with high V_{enc} PC VIPR and dual V_{enc} PC VIPR with 2D PC. Flow volume was measured in the AAO, DAO, MPA, SVC, and IVC. Peak velocity was only measured in the arterial system (AAO, DAO, and MPA) because peak venous velocities are often difficult to define. Biases between −6.25 and −1.50 mL, with a mean bias of −2.74 mL were found for total flow measured with dual V_{enc} PC VIPR. 95% confidence intervals for total flow measurements were between ±25.02 and ±29.80 mL with a mean of ±28.66 mL. Similarly, the mean bias for peak velocity comparisons was −6.45 cm/s with biases ranging between −10.68 and −3.99 cm/s. The 95%

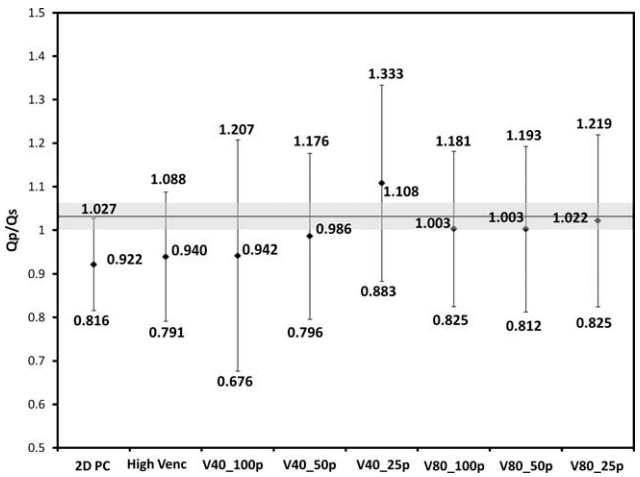

Figure 6. Measured average Q_p/Q_s ratios with error bars indicating ±1 standard deviation. The expected value of 1.03 ± 0.03 for normal volunteers is indicated by the solid line with the grey box representing 1 SD (21). Most techniques slightly underestimate Q_p/Q_s on average; however, all average values are within 10% of the expected Q_p/Q_s. For all techniques, the expected value of Q_p/Q_s is within ±1 standard deviation.

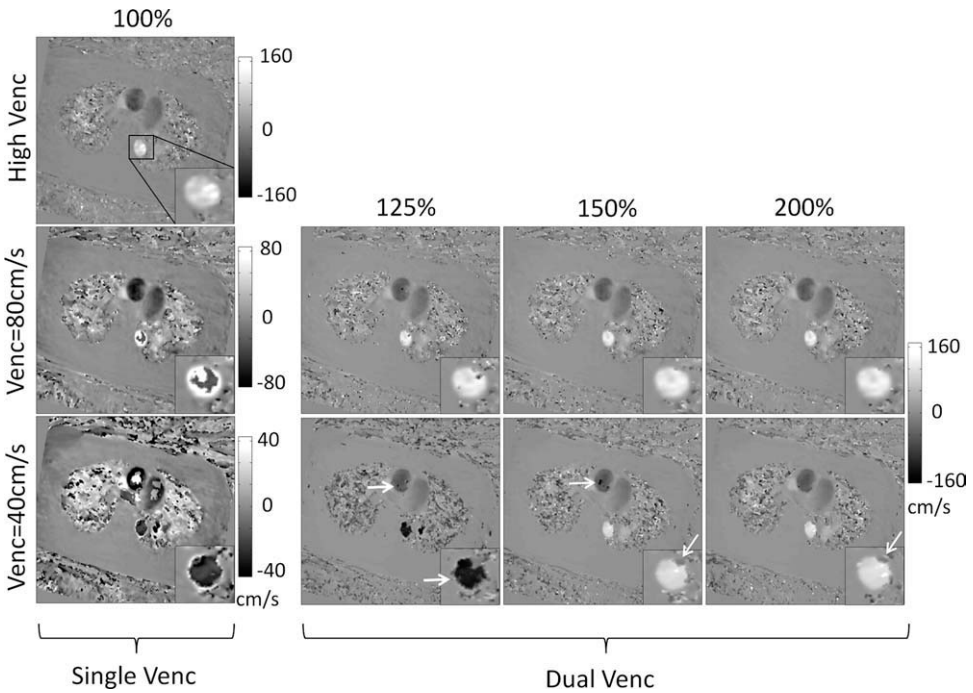

Figure 7. Example high, low and dual V_{enc} PC VIPR images. The inlay in each image shows the descending aorta. Black arrows point to locations of uncorrected velocity aliasing. Each column of images is labeled with the relative scan time, increasing from left to right (100% for a single V_{enc} PC VIPR acquisition). The dual V_{enc} PC VIPR images have the same dynamic range as high V_{enc} PC VIPR but with increased VNR. Phase errors decrease in dual V_{enc} PC VIPR when the scan time is increased.

confidence intervals for these measurements were between ±14.64 and ±20.39 cm/s with a mean of ±17.30 cm/s. The smallest biases on average were produced with the combination of a low V_{enc} of 80 cm/s corrected with 50% of the high V_{enc} acquisition. On average, the peak velocities and total flow zmeasured by dual V_{enc} PC VIPR were lower than those measured with 2D PC. This is most likely a result of the temporal filtering used in the PC VIPR reconstruction.

Figure 6 shows the average ratio of pulmonary to systolic flow (Q_p/Q_s) measured across all volunteers by each technique with standard deviations. This ratio in normal volunteers is 1.03 ± 0.03 on average (26). Most of the techniques slightly underestimate Q_p/Q_s; however, the average value is within 10% of the expected value.

Example AAO and SVC flow waveforms are shown in Figure 8. The ascending aorta waveforms agree well, although the peak flows are somewhat different. More discrepancy is seen between the IVC waveforms, however, they similarly agree well. The velocities in the IVC are low and, therefore, closer to the noise floor of the higher V_{enc} measurements.

Based on the RR interval analysis, it was found that the heart beat durations vary 5% in average and 11% at most within each acquisition. The average heart rate was found to be stable throughout the scan session as the average heart rates of the acquisitions varied by less than 4% between the scans and 6% the most.

In two volunteers, the ascending aorta flow waveforms measured with 2D PC were missing the peak systolic flow so ascending aorta flow measurements were not compared in those two volunteers. Prospective gating was used for 2D PC acquisitions so part of the waveform was missing. Similarly, two IVC waveforms measured with 2D PC were missing significant portions of the waveform so those volunteers were excluded from IVC analysis. In these cases, the missing portion of the waveform made it impossible to reliably compare the 2D PC and PC VIPR measurements. One volunteer moved during the PC VIPR scan with V_{enc} = 80 cm/s so that data was excluded from analysis. All other measurements were used for evaluation.

DISCUSSION

In this work, we have presented a thorough analysis of a dual V_{enc} PC VIPR acquisition and reconstruction technique that allows for a large gain in VNR with a modest increase in scan time for 4D PC-MRI. The addition of a high V_{enc} scan to an existing phase contrast scan led to a substantial increase in the velocity range over a scan with a single V_{enc} while maintaining the higher VNR of the low V_{enc} acquisition. Because the high V_{enc} scan was only used to correct phase errors in the low V_{enc}, this scan can be highly undersampled to reduce overall scan time. In time averaged phantom scans, large gains in VNR were achieved with small increases in scan time using a dV_{enc} acquisition and reconstruction. The measured VNR in a phantom was increased by a factor of three with only 5% additional scan time. In volunteers, the VNR gains achieved were less substantial than in phantoms due to complex aliasing patterns, noise, and a sparser signal distribution in phantoms. In vivo, we found a reasonable compromise between accuracy and scan time when combining V_{enc} = 80 cm/s with 25% of the high V_{enc} data, providing the VNR of a 80 cm/s acquisition while increasing the velocity range 100% .

For this study, we implemented a dual V_{enc} acquisition with eight velocity encodes: four high V_{enc} and four low V_{enc}. In theory, only seven-points are required for a 4D-PC dV_{enc} acquisition: a velocity compensated reference, three low V_{enc} and three high V_{enc} points. However, PC VIPR data were acquired with a

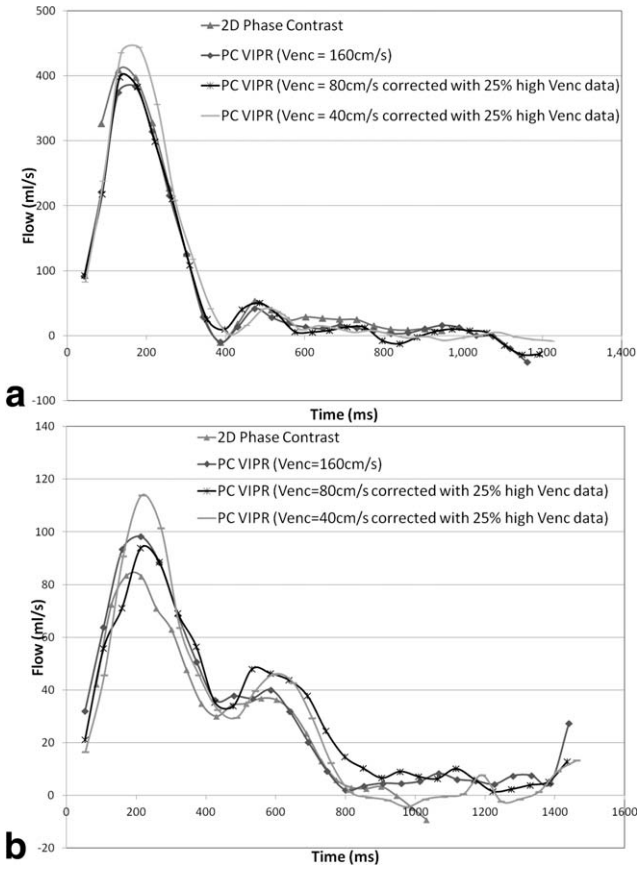

Figure 8. Representative flow waveforms acquired in (**A**) ascending aorta (AAO) and (**B**) superior vena cava (SVC) with 2D PC, balanced encoded PC VIPR and two dual V_{enc} acquisitions. The ascending aorta waveforms agree extremely well across all techniques. There is more variation between the waveforms acquired in the SVC, most likely due to slower blood flows in the venous system. Note, the 2D PC waveforms cover a smaller time interval because the 2D PC acquisition is prospectively gated and the PC VIPR acquisitions are retrospectively gated.

4-point balanced (Hadamard) flow encoding which requires smaller 1st moments compared with 4-point referenced encoding (27). Consequently, shorter TRs, shorter scan time, and improved temporal resolution can be achieved. However, Hadamard encoding is incompatible with a 7-point acquisition scheme. Depending on the V_{enc} setting, the possible advantage of time savings with 7-point reference encoding would be insignificant compared with an 8-point Hadamard encoding.

Another possible implementation for a dual V_{enc} acquisition would be to interleave the high and low V_{enc} scans. However, despite distinct benefits, there are costs associated with that approach as well. With an interleaved scan, the acquisition of the low V_{enc} data would have extended over a longer duration (up to twice as long), thereby possibly leading to greater errors from patient motion and physiological variation. Because the high V_{enc} scan is only used for phase unwrapping, these errors are much less likely to propagate to the final velocity estimation. Additionally, for a dual V_{enc} scheme, this would results in a decreased temporal resolution because seven or eight TRs are needed for a single phase encode (or unique radial projection) instead of four with the proposed implementation. Therefore, this scheme would result in a decreased temporal resolution leading to decreased accuracy in quantitative flow measurements.

A potential alternative to dual V_{enc} is the five-point encoding approach (16). A five-point encoding strategy corresponds to a balanced four-point acquisition with an added flow-compensated measurement. Johnson and Markl have reported 60% increase in VNR with a scan time increase of 25% by using a nonaccelerated five-point acquisition. Acceleration can also be applied to a five-point acquisition, and a 60% increase in VNR can be obtained with only a 1% increase in scan time. Thereby, a five-point velocity encoding approach allows for a shorter scan time than a dual V_{enc} acquisition. However, the gain in dynamic range is fixed and cannot be adjusted as it can be with a dual V_{enc} approach. With a dual V_{enc} approach, the VNR gain and scan time can be adjusted to specific applications.

In addition, several other methods have been proposed that could be used in conjunction with dual V_{enc} phase contrast to decrease phase unwrapping errors. Herment et al used spatial smoothness information from velocity images and magnitude signal for velocity estimation in dual V_{enc} 2D PC (28). The standard deviation over the cardiac cycle of the phase contrast image has been used as an indicator of which voxels to correct (29). Methods such as these could be used to improve VNR in dual V_{enc} images or reduce intermittent unwrapping errors at high undersampling rates.

The maximum VNR achievable in a dual V_{enc} acquisition is limited by various factors. As the low V_{enc} is lowered, the unwrapping becomes more sensitive to velocity noise in the high V_{enc} acquisition. This will result in phase unwrapping errors when the high V_{enc} image has errors from noise and/or undersampling. The achievable high V_{enc} undersampling rate decreases with an increasing high-to-low V_{enc} ratio. In time-resolved in vivo scans, we found an undersampling factor of 25% acceptable for a high-to-low V_{enc} ratio of 2 to 1. In time-averaged phantom scans, accurate results were achieved with a high-to-low V_{enc} ratio of 4 to 1 with a minimal increase scan time of 5%. Our data show that the achievable high V_{enc} undersampling factor is much higher for the phantom scans. This is due to the presence of more undersampling artifacts in the in vivo images from (i) using fewer projections by reconstructing individual time frames instead of an time average and (ii) a sparser signal distribution in the phantom.

Another factor that limits the effectiveness of a dual V_{enc} acquisition is errors in the low V_{enc} images. Because the low V_{enc} image is acquired with a large first moment, requiring large flow encoding gradients, it is more sensitive to intravoxel dephasing, acceleration errors, and signal loss from turbulent or unsteady flow. This can lead to errors in regions with large velocity dispersion, such as near vessel walls or distal to a stenosis. These effects limit the high-to-low

V_{enc} ratio that can be achieved. In addition, lower high-to-low V_{enc} ratios decrease the sensitivity of the phase unwrapping to errors in high V_{enc} acquisition caused by undersampling and noise. In this study, we found a high-to-low V_{enc} ratio of 2 to 1 provides a suitable balance between increased VNR and phase unwrapping errors. With this V_{enc} ratio, we were able to achieve an increase of 100% in velocity range of the low V_{enc} scan with only a 25% increase in scan time.

There are other potential limitations to this work. Phase errors could also arise from intra-scan patient motion. In most volunteers, the high V_{enc} and low V_{enc} scans were done at least 20–30 min apart with 2D PC measurements intersperse, and, therefore, some patient movement or physiological variation between the acquisitions is likely. In our cohort of volunteers, we found that variations in R-R intervals between scans were similar to variations of R-R intervals within single scans and, therefore, we believe patient heart rate variation did not affect the accuracy of results. In the clinical setting, much greater variability is expected due to pathology and patient disposition. The ultimate goal of an efficient dual V_{enc} acquisition is a single scan with back-to-back high and low V_{enc} encodings where the high V_{enc} data are undersampled for time savings yet do not reduce the accuracy of flow measurements. However, in this work the acquisition was accomplished in three subsequent scans to investigate the optimal high-to-low V_{enc} ratio and high Venc undersampling of a dual V_{enc} 4D PC-MRI acquisition. If we had acquired all the possible combinations of these factors with separate dual V_{enc} scans, the scan time would have been excessive.

In this study, parameters for a dual V_{enc} PC VIPR cardiac acquisition were investigated for imaging of the greater vessels in the chest. In future studies, the necessity to adapt settings to specific body regions has to be addressed. For instance, different scan field of view sizes could affect results because of variable inflow effects. Other factors such as vessel orientation and the presence of turbulent flows might also affect results.

In conclusion, we investigated an accelerated dual V_{enc} velocity reconstruction for 4D PC-MRI with radial sampling. With this approach, it is possible to increase VNR with modest increases in scan time. The efficacy and limitations of this acquisition were demonstrated in both, phantoms and volunteers. This approach is suitable to 4D MR flow measurements in vascular territories where quantitative flow analysis of vessels with a wide range of flow velocities are of interest as shown here for imaging in congenital heart disease. Other potential clinical applications include the hepatic and portalvenous system, arteriovenous malformations (AVM), aneurysms with jets and slow flow regions, and others. When adopting dual V_{enc} acquisitions to other vascular beds, the achievable acceleration might differ due to the vessel size, SNR, image contrast, and other factors.

ACKNOWLEDGMENT

We gratefully acknowledge GE Healthcare for their assistance and support.

REFERENCES

1. Bandettini WP, Arai AE. Advances in clinical applications of cardiovascular magnetic resonance imaging. Heart 2008;94: 1485–1495.
2. Koskenvuo JW, Jarvinen V, Parkka JP, Kiviniemi TO, Hartiala JJ. Cardiac magnetic resonance imaging in valvular heart disease. Clin Physiol Funct Imaging 2009;29:229–240.
3. Markl M, Harloff A, Bley TA, et al. Time-resolved 3D MR velocity mapping at 3T: improved navigator-gated assessment of vascular anatomy and blood flow. J Magn Reson Imaging 2007;25: 824–831.
4. Uribe S, Beerbaum P, Sorensen TS, Rasmusson A, Razavi R, Schaeffter T. Four-dimensional (4D) flow of the whole heart and great vessels using real-time respiratory self-gating. Magn Reson Med 2009;62:984–992.
5. Johnson KM, Gu T, Mistretta CA. 4D pressure mapping with time-resolved PC VIPR. In: Proceedings of the 13th Annual Meeting of ISMRM, Miami, Florida, 2005. (abstract 598).
6. Eriksson J, Carlhall CJ, Dyverfeldt P, Engvall J, Bolger AF, Ebbers T. Semi-automatic quantification of 4D left ventricular blood flow. J Cardiovasc Magn Reson 2010;12:9.
7. Johnson KM, Lum DP, Turski PA, Block WF, Mistretta CA, Wieben O. Improved 3D phase contrast MRI with off-resonance corrected dual echo VIPR. Magn Reson Med 2008;60:1329–1336.
8. Kvitting JP, Ebbers T, Wigstrom L, Engvall J, Olin CL, Bolger AF. Flow patterns in the aortic root and the aorta studied with time-resolved, 3-dimensional, phase-contrast magnetic resonance imaging: implications for aortic valve-sparing surgery. J Thorac Cardiovasc Surg 2004;127:1602–1607.
9. Wu SP, Ringgaard S, Pedersen EM. Three-dimensional phase contrast velocity mapping acquisition improves wall shear stress estimation in vivo. Magn Reson Imaging 2004;22:345–351.
10. Ebbers T, Wigstrom L, Bolger AF, Engvall J, Karlsson M. Estimation of relative cardiovascular pressures using time-resolved three-dimensional phase contrast MRI. Magn Reson Med 2001; 45:872–879.
11. Tyszka JM, Laidlaw DH, Asa JW, Silverman JM. Three-dimensional, time-resolved (4D) relative pressure mapping using magnetic resonance imaging. J Magn Reson Imaging 2000;12:321–329.
12. Salfity MF, Huntley JM, Graves MJ, Marklund O, Cusack R, Beauregard DA. Extending the dynamic range of phase contrast magnetic resonance velocity imaging using advanced higher-dimensional phase unwrapping algorithms. J R Soc Interface 2006;3:415–427.
13. Yang GZ, Burger P, Kilner PJ, Karwatowski SP, Firmin DN. Dynamic range extension of cine velocity measurements using motion-registered spatiotemporal phase unwrapping. J Magn Reson Imaging 1996;6:495–502.
14. Dyverfeldt P, Sigfridsson A, Knutsson H, Ebbers T. A novel MRI framework for the quantification of any moment of arbitrary velocity distributions. Magn Reson Med 2011;65:725–731.
15. Debatin JF, Ting RH, Sommer FG, et al. Renal artery blood flow: quantitation with phase-contrast MR imaging with and without breath holding. Radiology 1994;190:371–378.
16. Johnson KM, Markl M. Improved SNR in phase contrast velocimetry with five-point balanced flow encoding. Magn Reson Med 2010;63:349–355.
17. Lee AT, Pike GB, Pelc NJ. Three-point phase-contrast velocity measurements with increased velocity-to-noise ratio. Magn Reson Med 1995;33:122–126.
18. Johnson KM, Wieben O, Turksi P, Mistretta CA. Average and time-resolved dual velocity encoded phase contrast vastly undersampled isotropic projection imaging. In: Proceedings of the 14th Annual Meeting of ISMRM, Seattle, Washington, 2006. (abstract 2958).
19. Koladia KV, Pipe JG. Rapid 2D PC-MRA using spiral projection imaging. In: Proceedings of the 13th Annual Meeting of ISMRM, Miami, Florida, 2005.
20. Peters DC, Rohatgi P, Botnar RM, Yeon SB, Kissinger KV, Manning WJ. Characterizing radial undersampling artifacts for cardiac applications. Magn Reson Med 2006;55:396–403.
21. Barrett-Lee PJ, Dixon JM, Farrell C, et al. Expert opinion on the use of anthracyclines in patients with advanced breast cancer at cardiac risk. Ann Oncol 2009;20:816–827.
22. Chernobelsky A, Shubayev O, Comeau CR, Wolff SD. Baseline correction of phase contrast images improves quantification of

blood flow in the great vessels. J Cardiovasc Magn Reson 2007;9: 681–685.
23. Liu J, Redmond MJ, Brodsky EK, et al. Generation and visualization of four-dimensional MR angiography data using an undersampled 3-D projection trajectory. IEEE Trans Med Imaging 2006;25:148–157.
24. Anderson A, Wentland A, Johnson K, Wieben O. On the advantages of retrospectively gated radial acquisitions for cine phase contrast flow imaging. In: Proceedings of the 19th Annual Meeting of the ISMRM, Montreal, 2011. (abstract 4590).
25. Barger AV, Block WF, Toropov Y, Grist TM, Mistretta CA. Time-resolved contrast-enhanced imaging with isotropic resolution and broad coverage using an undersampled 3D projection trajectory. Magn Reson Med 2002;48:297–305.
26. Arheden H, Holmqvist C, Thilen U, et al. Left-to-right cardiac shunts: comparison of measurements obtained with MR velocity mapping and with radionuclide angiography. Radiology 1999; 211:453–458.
27. Pelc NJ, Bernstein MA, Shimakawa A, Glover GH. Encoding strategies for three-direction phase-contrast MR imaging of flow. J Magn Reson Imaging 1991;1:405–413.
28. Herment A, Mousseaux E, Jolivet O, et al. Improved estimation of velocity and flow rate using regularized three-point phase-contrast velocimetry. Magn Reson Med 2000;44:122–128.
29. Walker PG, Cranney GB, Scheidegger MB, Waseleski G, Pohost GM, Yoganathan AP. Semiautomated method for noise reduction and background phase error correction in MR phase velocity data. J Magn Reson Imaging 1993;3:521–530.